Final Project Report:

Rapid Non-contact Measurement using Multiple Point Laser Doppler Vibrometry for Health Evaluation of Rail and Road Bridges

by
Dr. Elizabeth K. Ervin, Principal Investigator
Dr. Vyacheslav Aranchuk, Co-principal Investigator
Dr. James Chambers, Co-principal Investigator

Civil Engineering, Mechanical Engineering, and the National Center for Physical Acoustics
The University of Mississippi
Box 1848
University, Mississippi 38677

NCITEC Project No. 2013-27

conducted for

NCITEC

January 2015

ABSTRACT

Measurement of dynamic responses to ambient stimuli can be used to evaluate as-built structural characteristics. These parameters can be used to determine the overall "health" of the structure; that is, the damage level and location can provide reliability information that aids infrastructure managers in maintenance decision-making. This type of inspection is most practical when it is non-destructive and swift.

In contrast to traditional vibration measurement systems, laser technology provides for rapid remote inspection. Laser Doppler vibrometers (LDV) have recently been used to capture non-contact vibration of bridges and are being used in an associated NCITEC project. In order to increase inspection speed to a practical threshold, multiple simultaneous laser beams will be employed. The National Center of Physical Acoustics (NCPA) at the University of Mississippi has been a leader in developing an instrument for parallel vibration measurements at multiple points. Results have been positive for such applications as landmine and tunnel detection. Civil infrastructure has an entirely different frequency range; massive structures with such low frequencies present a unique challenge.

In this project, a new method for structural vibration measurements on bridges will be implemented. The overarching idea is that parallel vibration measurements at multiple points using a multi-beam laser Doppler vibrometer will enhance non-contact bridge inspection technology. As proof of concept, the proposed effort will employ available equipment for measurements on a scale model bridge. The multiple laser beams will fan out to make parallel vibration measurements in multiple points on the model. Velocities of all interrogated points are measured and recorded simultaneously and are expected to enhance the accuracy of bridge mode shape calculation. Precise mode shapes lead to improved damage detection and thus more effective inspection results. The structural health algorithm will be modified based upon parallel measurements, and noise levels will be examined for practical feasibility.

Civil Engineering and National Center for Physical Acoustics personnel will work together to create a larger field of multi-beam vision and build a vibration isolation support system. Experiments will be conducted on an available scale model reinforced concrete bridge. The UM structural health program will employ advanced signal processing to extract mode shape data for damage detection. Output plots will visibly identify damage level and location and will be evaluated for detection accuracy as well as inspection practicality for bridge maintenance.

This project is expected to contribute to undergraduate/graduate courses as well as fund graduate students, which will result in advanced degrees. Technology transfer will include presented conference papers and submitted journal papers.

ACKNOWLEDGMENTS

TABLE OF CONTENTS

LIST OF TABLES

LIST OF FIGURES

INTRODUCTION

Structural health monitoring (SHM) of bridges is based upon measurement of dynamic responses to ambient stimuli, such as natural traffic or wind. Traditional vibration measurement systems use contact sensors that are bulky and difficult to mount. For example, damage detection using accelerometers requires access to bridge substructures, which may not be possible without lane or bridge closure. Inspection can take hours and may endanger inspector safety.

Rapid remote inspection is made possible by technological advances in laser technology. Laser Doppler vibrometers (LDV) have recently been used to capture non-contact vibration of bridges *(1-6).* Despite their ability to measure ambient vibration at selected locations on a bridge remotely, the commercial LDVs can only provide vibration information one point at a time. In order to increase inspection speed to a practical threshold, multiple lasers can be used; however, this induces problems with synchronizing the output velocity measurements.

Measurement at different points on a bridge can be implemented by point-by-point scanning of an LDV beam. However, the non-parallel nature of these measurements prevents accurate calculation of mode shapes that are used for assessing structural integrity and damage localization. The National Center of Physical Acoustics (NCPA) at the University of Mississippi has been a leader in developing an instrument for parallel vibration measurements at multiple points; for example, ground vibration measurements have been used in acoustic landmine detection *(7).* The product of such work was a mobile acoustic/seismic confirmation sensor: the cart system was successfully used in experiments at landmine fields *(8-12).* The same system has been also used for passive acoustic tunnel detection *(13)* and detection of a vehicle obscured by a forest canopy *(14,15).*

A variety of acoustic applications has shown LDV equipment to be effective in the acoustic frequency range. However, civil infrastructure has an entirely different frequency range; massive structures have such low frequencies that noise is difficult to overcome. Parallel LDV equipment has never been used for bridge applications, but the potential for overhauling rail and road bridge inspection as known today. This effort will enhance non-contact bridge inspection technology by rapidly and remotely capturing simultaneous vibration measurements in a linear array capture an object's surface motion.

These simultaneous velocity measurements at multiple points are expected to enhance the accuracy of bridge mode shape calculation. Precise mode shapes lead to improved damage detection and thus more effective inspection results. The structural health evaluation program has been generated through the UM2012_24 project. Single point measurements are underway, but concern has developed about practical inspection speed; slow single point measurements on a bridge could generate lengthy lane closures. Parallel measurements would allow a single setup location off the bridge, similar to surveying equipment. The structural health algorithm will be modified based upon parallel measurements, and noise levels will be examined for practical feasibility.

The main technical challenge is that the laser beam system must be evaluated for the large scan area of civil infrastructure. The multi-beam instruments must be configured to accommodate the slab spread of the scale model bridge. This is the first step to applying this state-of-the-art technology to larger structures. Then the standoff distances over which the lasers measure must be increased, which will affect the lasers' angles. Additionally, the

expensive instrument(s) must be securely supported for measurements in multiple directions. These measurements will ensure capture of all structural mode shapes and will require the design and construction of a versatile supporting frame. A final concern is the equipment cost for any department of transportation; vibrometer settings will be optimized to apply to as many different structures as possible, increasing cost effectiveness.

OBJECTIVE

This work intends to improve damage detection in bridge inspections via parallel non-contact vibration measurements. In contrast to traditional contact measurements, laser technology provides for rapid remote inspection. A specific challenge of this non-destructive testing technique is low frequency sensitivity, but the advantage of decreased inspection time warrants further investigation. As a proof of concept, the proposed effort will employ available multi-beam LDVs (laser Doppler vibrometers) for measurements on a 1:12 scale model bridge built through the NCITEC UM2012_24 project. Initially, a linear array 16-beam LDV system was to be employed, but instead three single point LDVs were used due to scope reduction on 6/5/2013. This will still serve the purpose of evaluating the accuracy and efficiency of simultaneously parallel non-contact vibration measurements.

The three primary activities of the project are individually detailed here as well as separated in the Methodology and Results sections.

1. Construct Instrumentation System (January 2014 - May 2014).
Three single point LDVs will be simultaneously employed. Their base isolation is essential to obtain absolute measurements on the bridge. A floor-mounted frame will be designed to reduce measurement noise caused by ambient vibration. Measurements will be taken underneath the bridge in the vertical direction. Data will be captured by the available National Instruments USB CompactDAQ system.

2. Conduct Experiments on Scale Model Bridge (May 2014 - July 2014)
At the onset of testing, the scale model bridge will have been in place for one year. New multi-beam baseline data will be captured and compared to previously captured single point data. The sensitivity of the multi-beam method will be evaluated, and noise levels will be analyzed in order to assess practical inspection feasibility.
Production runs will include multiple series of experiments using multiple beams. Settings will be examined for their effects on noise levels. Vibratory velocity will be captured and used to evaluate dynamic characteristics of the scale model bridge. Attempts will be made to capture both horizontal and vertical components of vibration. The measurements will be repeated for a case with a defective substructure component.

3. Develop and Test Damage Detection Code (June 2014 - December 2014)
The basic damage detection algorithm began by UM2012_24 will be augmented to accommodate new multi-beam data format. This MATLAB code will perform all necessary signal processing to extract mode shape data for damage detection. An algorithm for speckle noise mitigation may need to be incorporated. Output plots will visibly identify damage level and location using at least twelve different detection schemes. Results will be evaluated for detection accuracy as well as inspection practicality for bridge maintenance.

SCOPE

Technical limitations of this project stem from budget restrictions in addition to structural limitations. Damage indicators cannot be expected to work identically for all structures or even all bridges. No developed methodology can be valid without application to a variety of infrastructure. On-going UM work is further analyzing each indicator and its effectiveness in identifying damage present in various materials and geometries in order to draw broader conclusions.

The long-range hypothesis yet to be proven is that separate classifications of structures will require different damage detection metrics. Once the most effective indication method for a structural system type has been determined, the safety threshold can be determined. This method and its associated threshold parameters will aid decision-making on maintenance based upon structural condition. The ultimate goal is to limit the total damage caused by all abnormal events as well as aging throughout the structure's lifetime to an allowable "safe" threshold.

The technical scope is also limited to overall health (and global modes), so subsequent local inspection may be indicated. Locating of potential damage is still extremely valuable for more pointed inspection and maintenance. To be feasible, the employed health evaluation technique should be more sensitive, reliable, and cost-effective than currently employed visual inspection methods.

Another technical restriction in health evaluation is that large damage events may alter the modal response of the structure such that subjective modal comparisons become even more uncertain. This means that mode shapes calculated from large damage events cannot always be visually compared to baseline mode shapes due to coupling of modes which can cause extreme visual differences between the two cases. Closely spaced modes can also prove troublesome since large modal peaks that can dwarf smaller peaks. There is also a lower frequency limitation based upon instrumentation and post-processing; this can interfere with massive infrastructure, which have low resonant frequencies.

At this time, the developed structural health program is limited to internal use only. The name has been trademarked by the University of Mississippi, and the next step after some additional development will be software licensing. Proposals have been submitted to allow and encourage government use of such software to augment inspections.

In this project, a new method for structural vibration measurements on bridges will be implemented. The overarching idea is that parallel vibration measurements at multiple points will enhance non-contact bridge inspection technology. The technique will eventually advance to implementation on a bridge at a distance on the order of hundreds of meters. Figure 1 shows a concept of bridge inspection. The laser beams are configured in a linear array and are directed onto different locations of the bridge. The devices can be located either under the bridge and measure vertical vibrations, or it could be mounted on the ground away from the bridge and measure horizontal vibrations (shown).

Figure 1. Concept of enhanced bridge inspection; I-55 over I-74 in Bloomington, IL
(16).

METHODOLOGY

In this section, the methodology behind the three primary activities will be discussed.

1. Construct Instrumentation System

As a quick review, the scale model bridge in the NCPA building was designed by graduate students and constructed by undergraduate students. It took 47 days to build forms and set rebar, and then concrete was poured in April 2013. After a 37-day cure time, the bridge was assembled via forklift. It is approximately 1:12 scale of an on-campus bridge (Eastgate Bridge). The university photographer took the photo of impact testing below in Fall 2013.

Figure 2. Impact hammer testing with Steven Worley and labmate Farhad Sedaghati.

Weighing approximately 1270 pounds, the 60"x42"x6" center slab is the target of the vibration testing. A 12-pound PCB sledge hammer impacts the wood block on the bridge, inducing multi-dimensional vibrations. A Dytran tri-axial accelerometer on a level deck pad at the center point (Point 28) was used as a stationary control during all testing.

Despite their ability to measure ambient vibration at selected locations on a bridge remotely, the commercial LDVs can only provide vibration information one point at a time. In order to increase inspection speed to a practical threshold, multiple lasers can be used. Model PDV100 by Polytec, Inc., three single point LDVs were used to take non-contact velocity measurements. These three sensors increased the field of vision and reduced test time by three.

Shown in Figure 3, the preliminary test setup captured horizontal vibrations. Required optical equipment included an isolated table with mounted sliding beams. The purpose was to

debug any instrumentation concerns and determine data acquisition settings. A National Instruments CompactDAQ records the signals via NI LabVIEW and synchronizes the output velocity time histories. The resulting comma-separated text files are loaded into the MATLAB structural health algorithm for post-processing.

Figure 3. Preliminary test setup with three LDVs shooting target slab vibrations.

Vertical Z-direction vibrations will provide the characteristic beam bending modes of the slab. In order to capture this direction, a frame had to be built to insert under the bridge. The base isolation of the LDVs is essential to obtain absolute measurements. The floor-mounted frame will reduced measurement noise by a factor of 10 versus attaching the frame to the footings. Figure 4 presents a schematic of this overall setup. Vibration of all three interrogated points are measured simultaneously and recorded by the data acquisition system into computer memory.
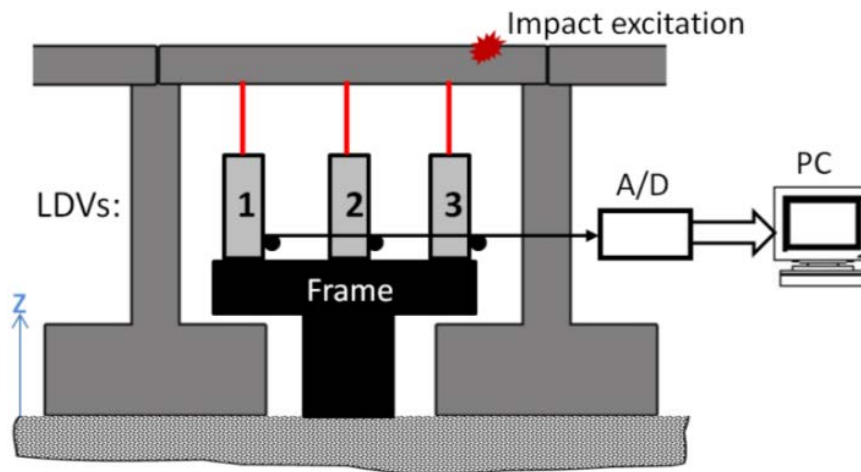
Figure 4. Schematic diagram of vertical instrumentation.

2. Conduct Experiments on Scale Model Bridge

Production runs included the two cases sketched in Figure 5. The concrete connections represent the "undamaged" case as a basis for comparison. To create a "damaged" case, a 1/16-inch thick 40-durometer Buna-N rubber bearing was inserted at the top of the right t-shaped pier. Laser measurements were made for each case at the forty-five points shown in Figure 6. Note that the boundary points on the piers could not be captured as there was no space underneath the slab.
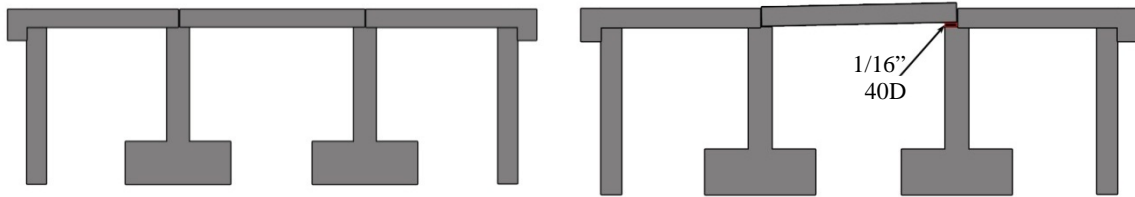
Figure 5. Baseline with concrete connections (left) and damaged case with one rubber bearing (right).
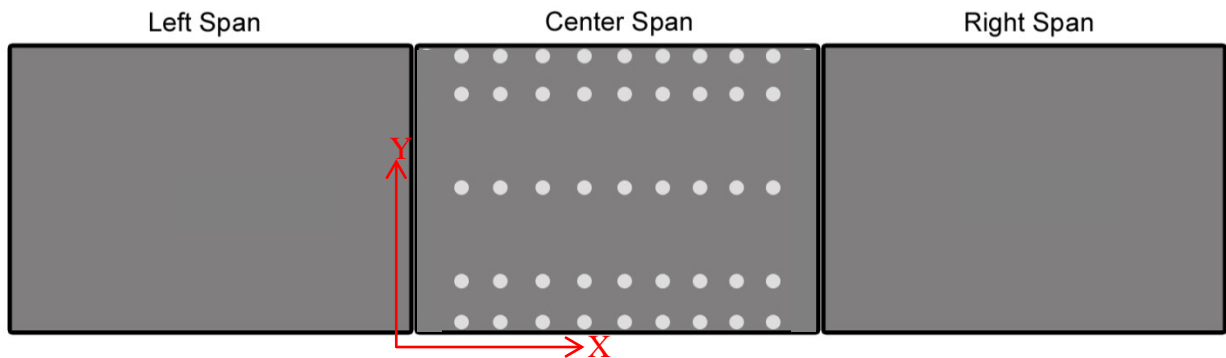
Figure 6. Forty-five data points measured underneath the center slab via laser velocity measurement.

The three Laser Doppler Vibrometer apparatus used to make simultaneous non-contact velocity measurements sits underneath the bridge in Figure 7. The measurement grid of 45 points underneath the slab are fitted with retro-reflective tape. As a hammer strikes the bridge inducing three-dimensional excitation, the LDVs measure the simultaneous vibration response in real-time for three different points.

Figure 7. Experimental setup in place underneath the center slab.

The top-down view of the apparatus shown in Figure 8 utilizes three optical rails and corresponding sliding carriers to allow three single-point LDVs, mounted to an optical breadboard, to freely slide in the X and Y directions. This large range of motion allows for quick and easy measurements: fifteen sets of three laser measurements were taken to span the entire slab. The optical rails sit atop a raised optical breadboard to elevate the rails, and subsequently the LDVs, above the base of the bridge so that they can be moved along the full depth of the top slab.

The side view of the apparatus in Figure 9 shows how the horizontal LDVs capture vertical measurements. The LDV beams are directed upwards by 45° mirrors in the Z direction, allowing for vertical beam targeting. Additionally, since the mirrors are mounted on the same breadboard as the LDVs, there is no realignment needed after each set of

measurements. Only macro-movement of the breadboard along the rails is needed. Figure 7 shows the three beams on the bottom of the bridge deck.
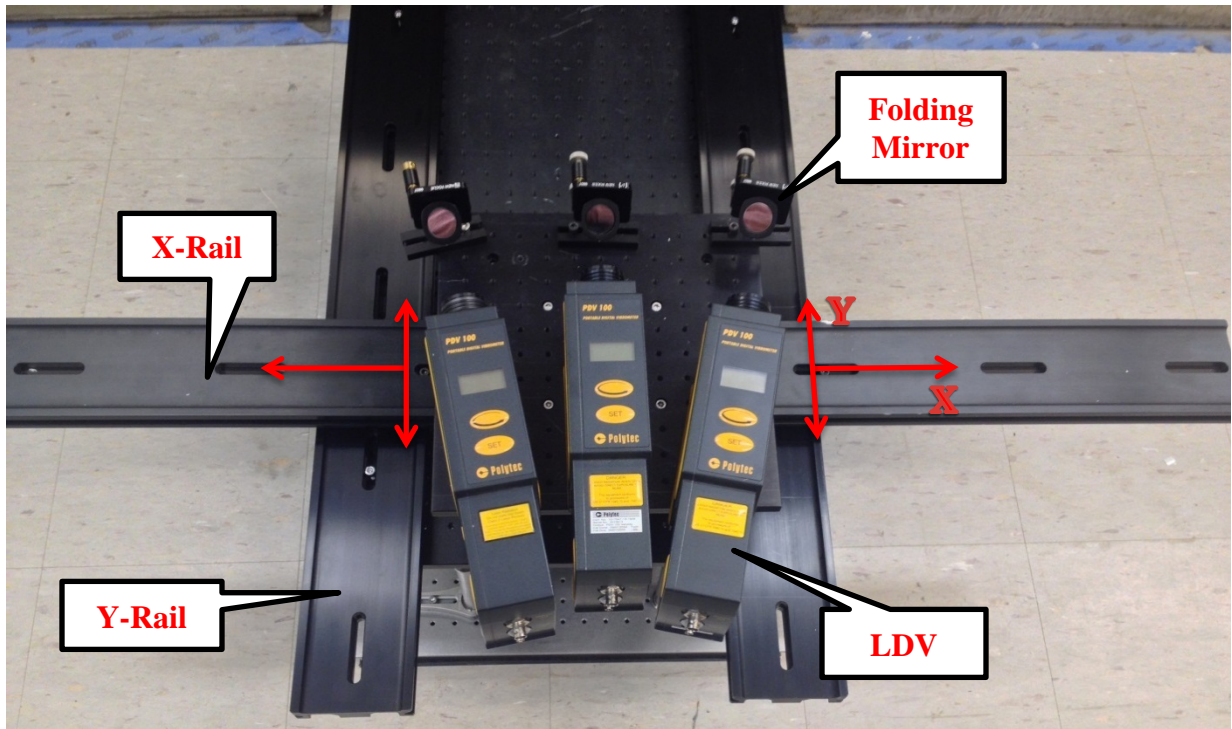
Figure 8. Experimental setup, top view.

Figure 9. Experimental setup, side view.

A test in progress is shown in Figure 10. Approximately fifty hammer hits were required to complete all necessary non-contact vertical slab measurements. If a traditional contact single-axis accelerometer method had been used, 150 hammer hits would have been required. Thus, in addition to the remote sensing advantage, effort has been reduced by one-third, a valuable time savings for inspectors. Note that the same number of hammer hits would be required to equate tri-axial accelerometer use.

Figure 10. Impact test in progress.

3. Develop and Test Damage Detection Code

Over the past several years, Dr. Ervin and her team completed the development of a comprehensive structural health program entitled SHE™, or Structural Health Evaluation™. The flowchart is provided in Figure 11. There are four major modules: 1) input, 2) modal analysis, 3) health algorithms, and 4) output. The input is dominated by numerous data types and formats that can be provided for spatially diverse structures. Time history input is any comma-separated text file. Furthermore, the degrees of freedom and their locations must be recorded universally. Modal decomposition is a simple concept but one that is difficult to automate: to have full control of the algorithms, the team developed their own code. The team built one integrated program that employs several health algorithms. The user then correlates two modes upon which numerous structural health algorithms are applied. Visual output was completed for user ease: color-coded output is displayed to the screen, and these plots were provided throughout this report.

After data capture, the time histories obtained from the LDVs are loaded as this MATLAB code's input. Signal processing then commences to extract mode shape data for later damage detection. The first step is that fast Fourier transforms (FFTs) are calculated to generate frequency response functions. Modal peaks are then identified: note that natural frequency identification and mode correlation can be quite subjective: mode shape plots assist in these tasks, but time must be expended to analyze each potential resonance.

Figures 12 through 15 provide frequency response functions for gathered data. Each figure contains only vertical Z direction data, including the tri-axial accelerometer located at the slab's center, Point 28. The abscissa contains the frequency range of interest in structures: 0 to 50 Hertz (Hz) is considered "low," 50 to 200 Hz is "medium," and 200 to 300 Hz is "high." Neither g nor mm/s, the ordinate is FFT amplitude, and it is unit normalized for each trace's maximum up to 300 Hz. The same NI CompactDaq data acquisition settings were used throughout.

For the baseline case with concrete connections, Figures 12 and 13 present the frequency response functions for the midpoint, Point 28. Three traces are shown: the control is the red trace of the accelerometer on the deck surface. The other traces are the LDV measurements from underneath the slab at Point 28; the green trace has been low-pass filtered while the blue trace is unfiltered. Figure 12 presents the full frequency range of interest while Figure 13 presents the low range response, less than 50 Hz, shown on a logarithmic scale to exaggerate differences.

Recall that amplitudes are arbitrary due to normalization. The medium range response reveals similar resonances near 121 Hz, and other peaks are consistent. The peak around 60Hz appears only in the LDV responses and thus is most likely caused by line power. Harmonic interference could also be occurring near 120 Hz. The peak responses appear well correlated for the high frequency range, greater than 300 Hz. However, the low frequency range shows significant differences.

A major LDV setting, filtering has been examined for its effect on frequency content. A low-pass filter prevents frequencies above a certain threshold (here, 1 kHz) from causing measurement noise. However, filter use can induce artifacts in the data, such as shifting peaks, even at frequencies less than the selected threshold. Figure 13 shows that this is evident in the LDV responses (green vs. blue). Some peaks at LDV spectra, for example at 13 Hz and 19 Hz, could be caused by vibration response of LDV setup components, such as

mirror mounts and rails.

　　Additionally, the accelerometer frequency content varies from both LDV responses. This difference in peak locations could be caused by sensor location. That is, the accelerometer was located on the deck while LDV shot at the bottom of the slab.

Geometric Properties

User input – build the structural model by editing a function file to define locations, members, and sensors.

Prior Sensor Data

Two Modal Decompositions

Current Sensor Data

Baseline case – interactive – select and store mode shapes, natural frequencies, and FRF Magnitudes/Real/Imaginary.

Damaged case – select and store mode shapes, natural frequencies, and FRF Magnitudes /Real/Imaginary.

Mode Coordination

Selection of Mode Pairs – interactive – plot mode shapes vs. each other for damaged and undamaged case – do they compare?

Indicator Algorithms

Store values for each indicator and algorithm that will be used for plotting as well as the large matrices such as flexibility that can be used or viewed later.

Output

Visualization – graph output for each indicator and its corresponding algorithms for decision making.
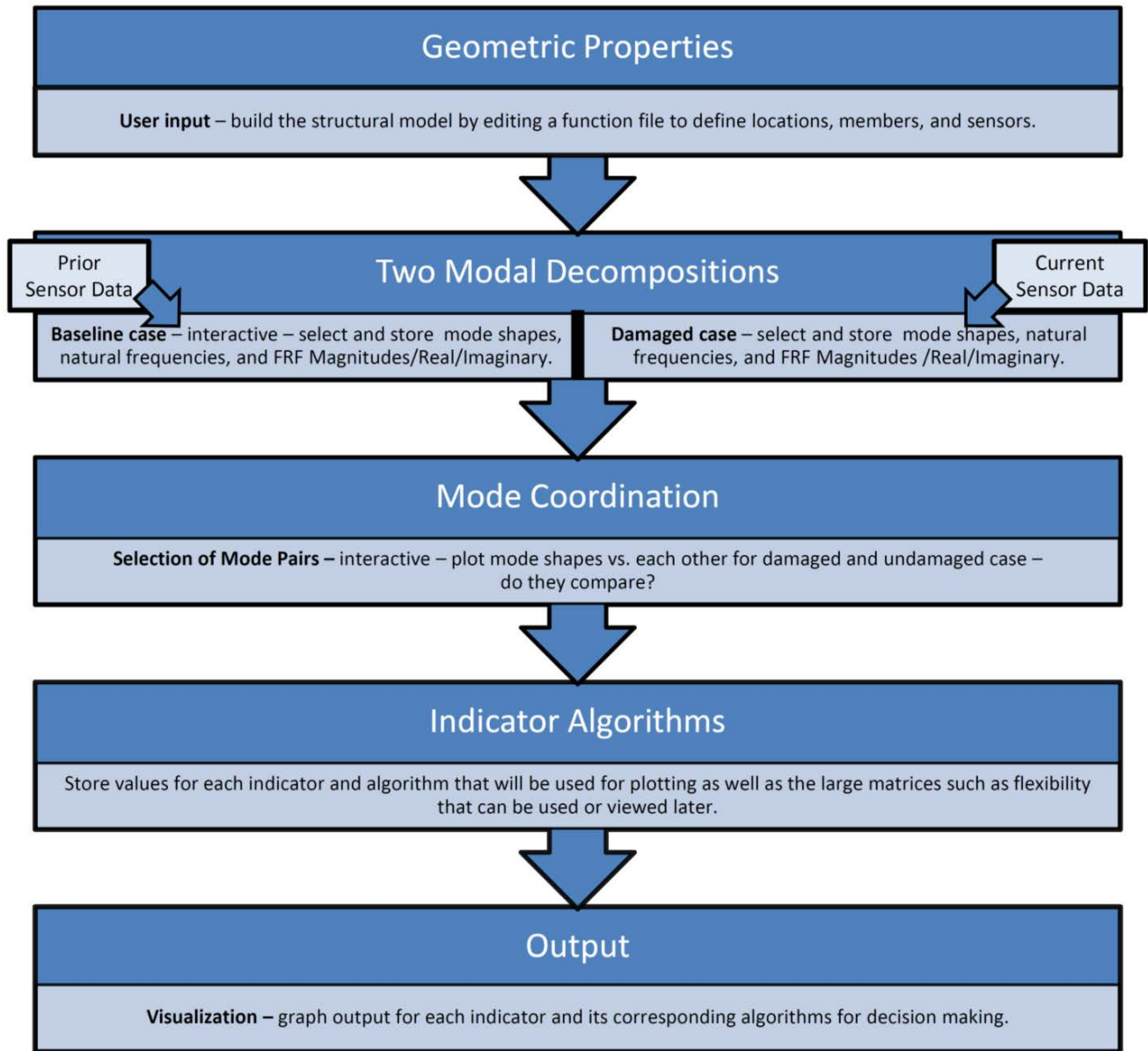
**Figure 11. SHE^{TM} flowchart.**

For the baseline case with concrete connections, Figure 14 presents the averaged frequency response functions using all 45 points. Following the non-contact tests, a tap test was performed by relocating the accelerometer for each hit, and only the Z-component signal was used herein.

The unfiltered LDV signal better matched the low frequency response: peaks were identified at 17, 25, 31, and 40 Hz. The filtered resonances are lower than others and thus will be disregarded in the future. That is, the LDV should be used without a filter. The difference may also be caused by LDV response to impulse loading, such as the hammer impact. These single point Polytec LDVs are normally used for continuous vibration signals, and their application for impact measurement may result in artifacts.

For the damaged case with one rubber bearing, Figure 15 presents the averaged frequency response functions using all 45 points. Following the non-contact tests, a tap test was performed by relocating the accelerometer for each hit, and only the Z-component signal was used herein.

The difference in sensor sensitivity is evident in Figure 15. The normalization focuses on the medium range for the LDV, but closer examination reveals reasonably close frequency content. The LDV measurements certainly have more noise, especially at low frequencies which changed significantly from the baseline. In fact, the LDV response is difficult to identify resonant peaks, so post-processing is underway. The LDV response does show interference at 60 Hz, the power line frequency, that the accelerometer does not indicate. Additionally, LDV peaks near 120 and 175 Hz appear to be shifted upward from accelerometer results. High frequency results greater than 200 Hz appear inconclusive.

In short, the differences in the frequency content do not indicate success or failure of the non-contact remote inspection method. While the natural frequencies and mode shapes are valuable assessment tools, the true metric will be the differences in the damage detection plots. These figures will visibly identify damage level and location using at least twelve different detection schemes. Results will be directly contrasted for traditional accelerometer data versus the non-contact multi-beam LDV data. Thus, the focus of the project is generating the damage detection plots and evaluating the sensitivity of the multi-beam method.
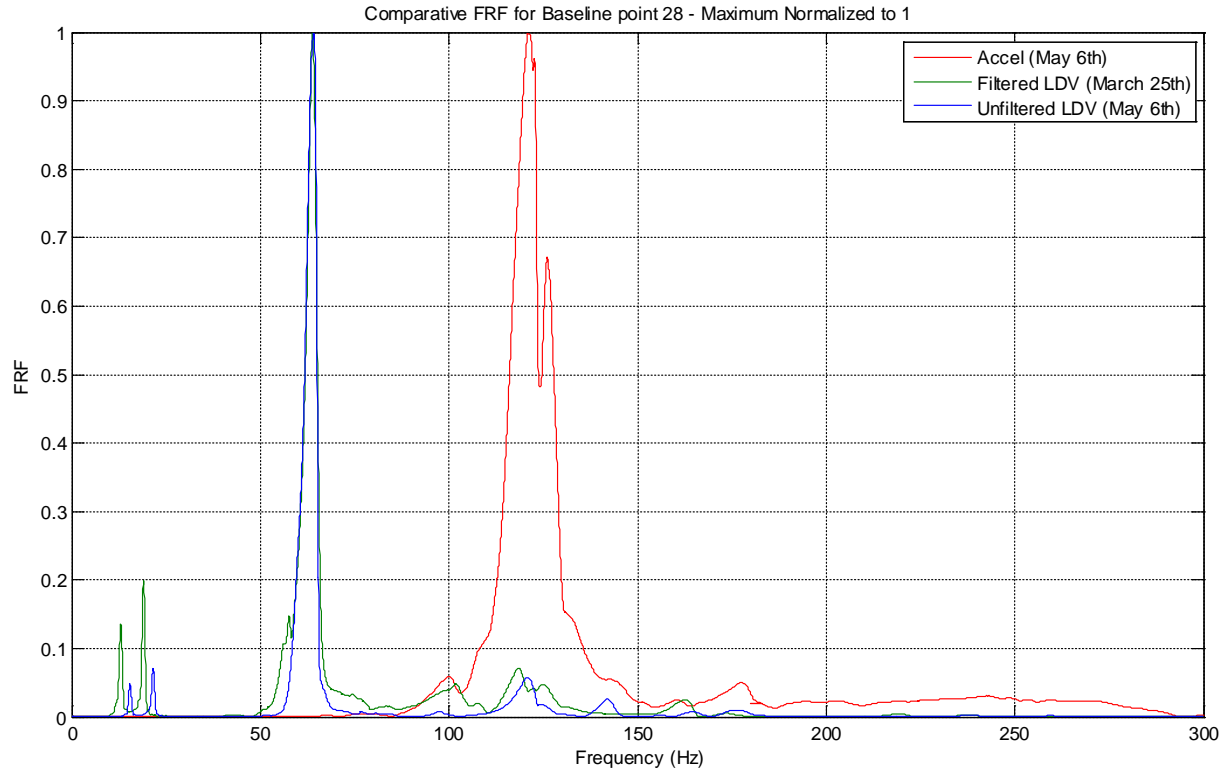
Figure 12. Direct comparison of frequency response functions for Point 28.
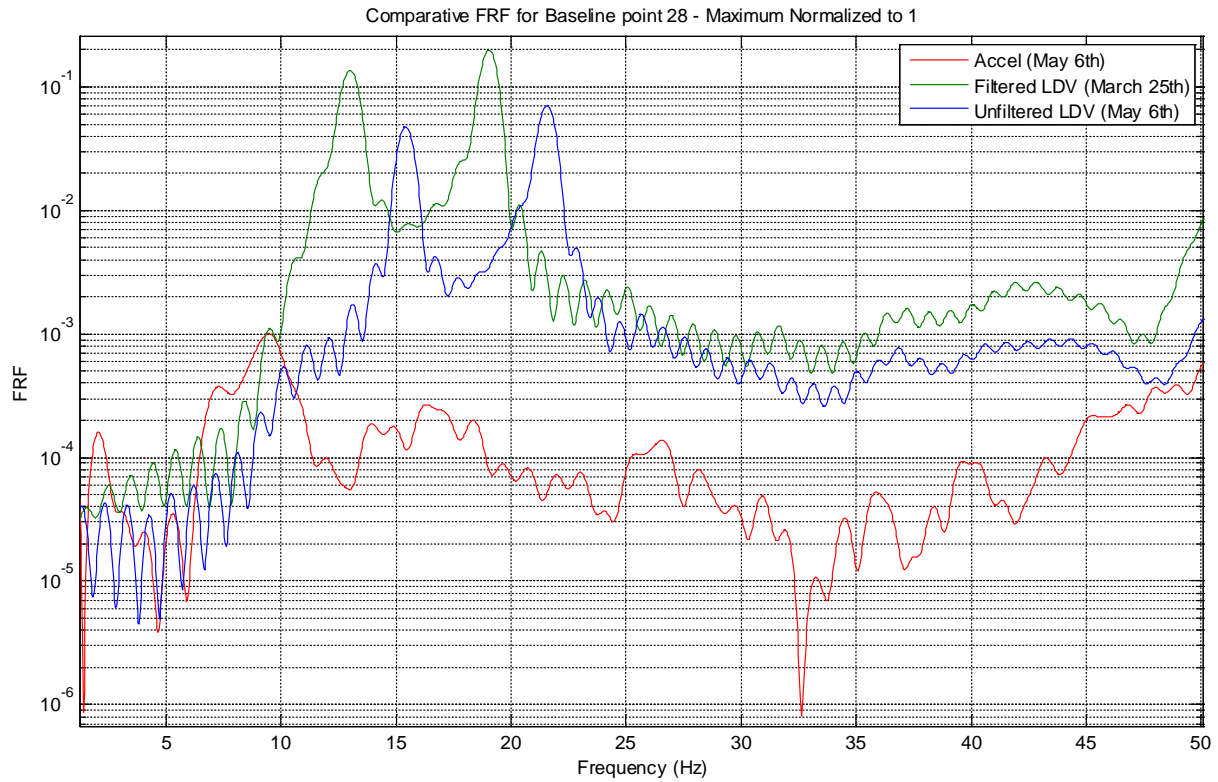
Figure 13. Direct comparison of frequency response functions for Point 28: 1 to 50 Hz, log scale.
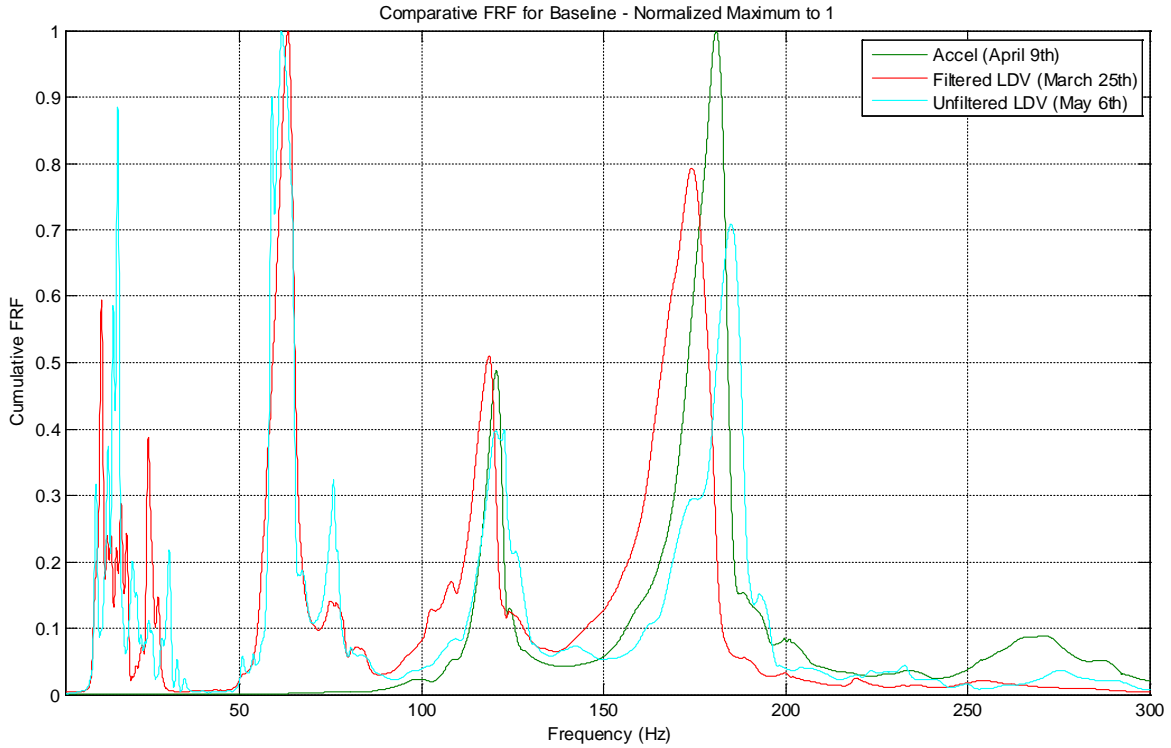
Figure 14. Averaged frequency response functions for contact accelerometer vs. non-contact LDV data: baseline case.

Figure 15. Averaged frequency response functions for contact accelerometer vs. non-contact LDV data: damaged case.

DISCUSSION OF RESULTS

In this section, Activity 3's results of the structural health damage detection program are presented for the scale bridge model using multiple LDVs.

Production runs included two cases: concrete connections as the "undamaged" case and a rubber bearing on the right pier as the "damaged" case. Laser measurements were made for each case at forty-five point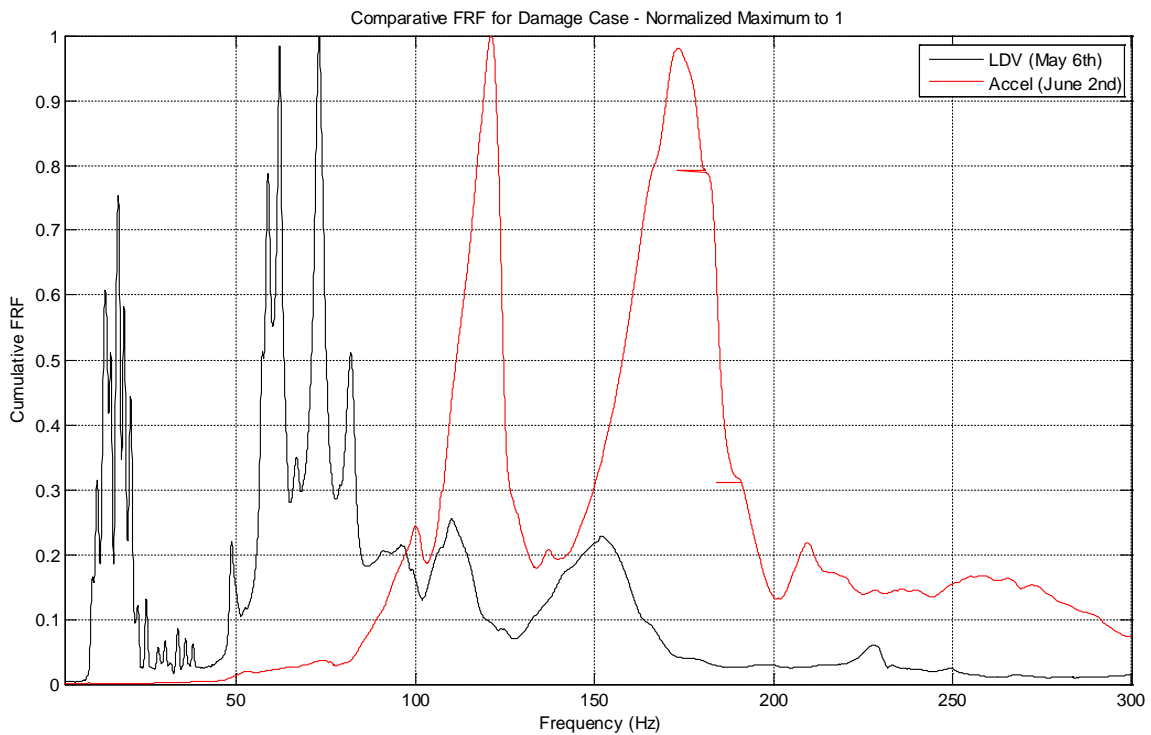s, omitting boundary points. The three Laser Doppler Vibrometers made simultaneous non-contact velocity measurements from underneath the bridge. As a hammer strikes the bridge inducing three-dimensional excitation, the LDVs measure the simultaneous vibration response in real-time for three points at a time.

The wireframe drawing of the sensor network was constructed. Then the process of loading the obtained time histories into the damage detection algorithm began with signal processing to extract mode shape data. The fast Fourier transforms (FFTs) were calculated to generate frequency response functions LDV filtering was turned off due to peak shifting. For the baseline concrete connections, comparison of the same data points revealed different peaks for the same impact. The LDV's velocity measurement and accelerometer's g-measurement provide different low frequency response, which is vital for massive civil infrastructure.

The next step in damage detection was to identify modal peaks for both the LDV data and the accelerometer data. This was only directly comparable in the vertical z-direction; however, tri-axial accelerometer data was used to assist in identifying mode shapes via the other two directions. The results both damaged and undamaged cases were independently investigated.
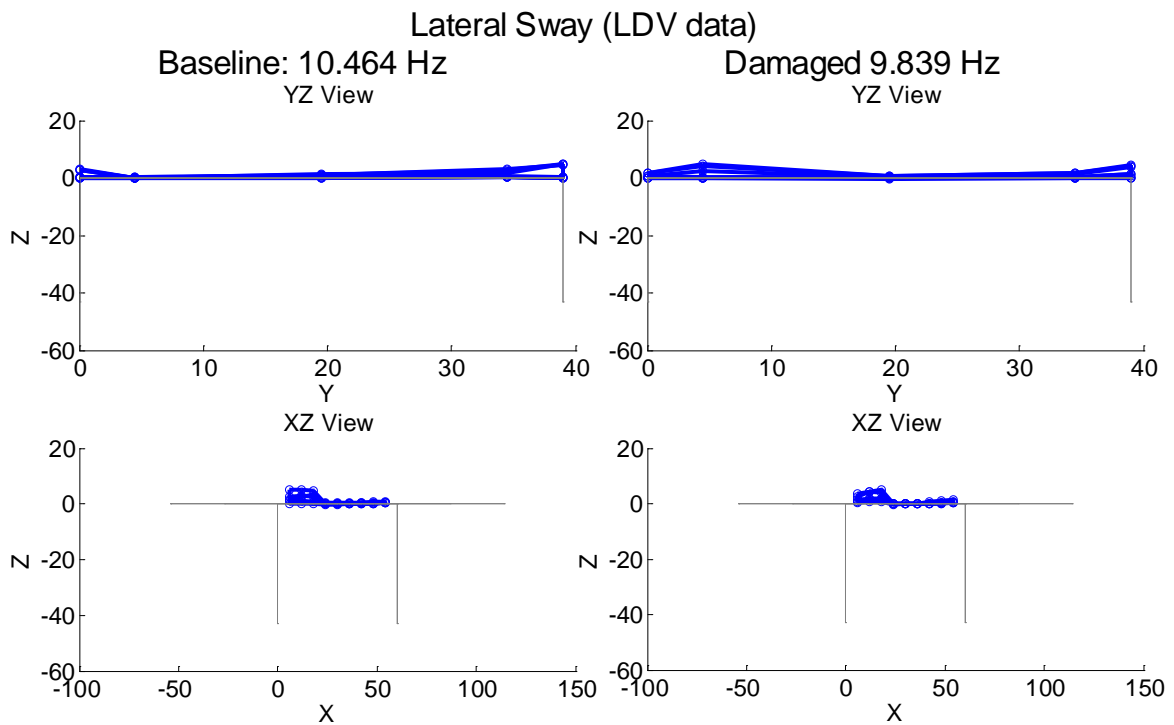
The modal decomposition process resulted in numerous modes. FFTs were calculated using 2^{18} points, permitting a frequency resolution of 0.039 Hz in the frequency range of 0 Hz to 300 Hz. The accelerometer data sets produced 34 dominant peaks for the baseline and 31 for the damaged case. Examination of strictly the z-direction baseline accelerations still revealed 27 modes.

The LDV data sets produced 64 unique peaks for the baseline and 55 for the damaged case. The LDV signals provided nearly twice the potential modes due to the increased sensitivity and noise. This required more personnel judgment for modal identification, specifically in the lower frequency range (less than 100 Hz).

In fact, there existed few comparable modes between the LDV and the accelerometer. This was partially due to the lack of in-plane measurement: the laser can only measure along its beam. For example, the lateral translation mode is shown in Figures 16 and 17: the in-plane XY view is required to view the y-direction sway (Figure 16). Considering only z-direction is measured, this view is not available for LDV measurements from under the bridge, and normalization of each view further obscures any y-direction motion (Figure 17). The associated dominant peaks occur at 9.336 Hz for the cumulative acceleration signals and 10.464 Hz for the cumulative velocity signals. The 12.08% difference for this fundamental frequency was the greatest: all higher frequency peaks were within ±1.25%. It is interesting to note that the frequency of the lateral sway mode actually increased 3.77% with damage for the accelerometer data; this is possible due to nature of concrete contact surfaces. Since damage softens structural stiffness, a decrease in natural frequency is expected, as in the LDV result of -5.97%.

Lateral Sway Mode

Baseline: 9.336 Hz   Damaged: 9.688 Hz
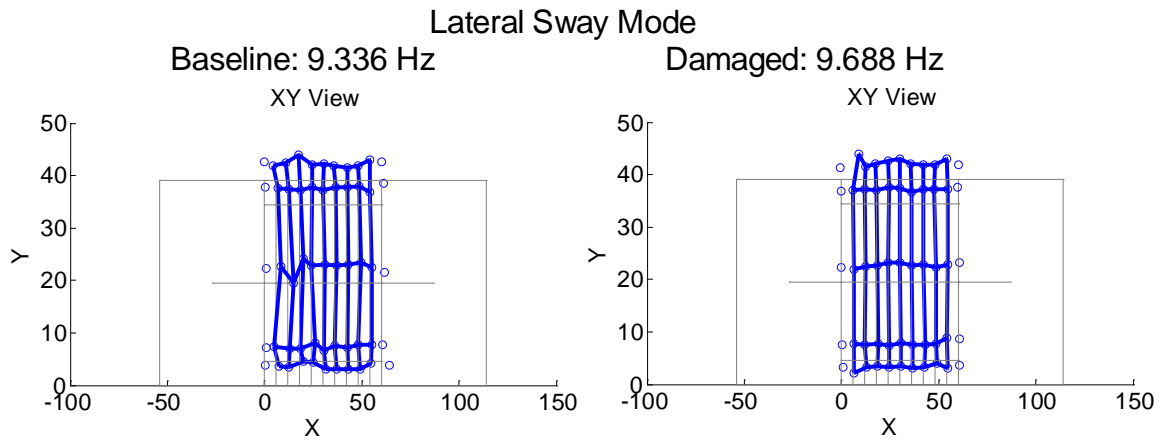
Figure 16. In-plane plot of the dominant sidesway mode using tri-axial accelerometer data.

Lateral Sway (LDV data)

Baseline: 10.464 Hz   Damaged 9.839 Hz

Figure 17. Planar plots of the sidesway mode using single axis LDV data.

Coordination of baseline to damaged modes is required for the next SHE^{TM} step. This is difficult without tri-axial data. Thus, the value of any comparison of the LDV to accelerometer modes is minimal. Additionally, the LDV setup is unable to provide time histories for the ten boundary points, creating more uncertainty in mode shape boundary condition.

However, data comparison between the LDV baseline to LDV damaged case is valuable: as in Figure 17, coordinating baseline to damaged is possible. The same is true for data comparison between the acceleration baseline and the acceleration damaged case. Thus, the true success metric is the damage detection plots. These figures visibly identify damage level and location, and they can be directly contrasted for traditional accelerometer data versus the non-contact multi-beam LDV data. This is used to evaluate the sensitivity of the multi-beam method.

Damage Detection Results: Tri-Axial Accelerometer Data

The cumulative frequency response functions (FRFs) are provided in Figure 18. These traces are the summation of all 55 data points in all three channels, or 165 time histories. The damaged trace's peaks have lesser magnitude and are "softer," demonstrating that more damping has been introduced into the system.
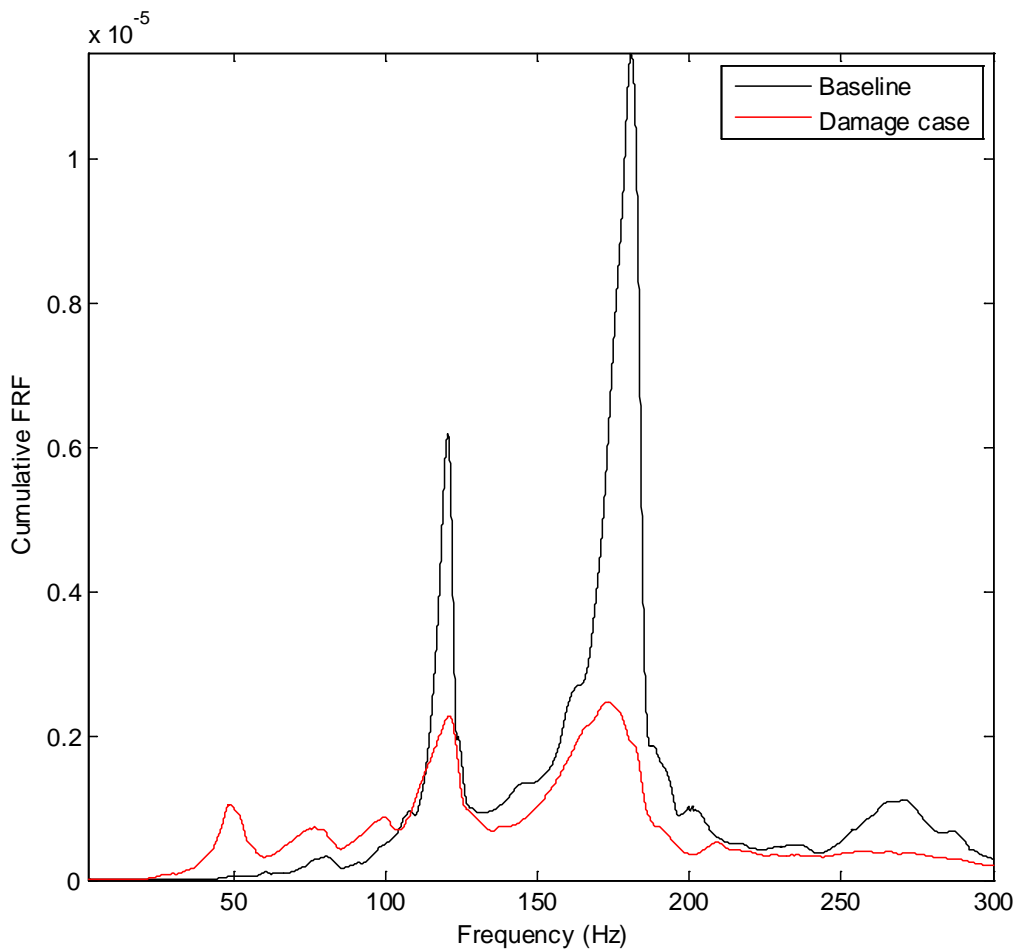
Figure 18. Non-normalized cumulative FRFs using tri-axial accelerometer data.

Comparison of the mode shapes reveals the coordinated modes of Table 1. The baseline mode shapes have been meticulously compared to the damaged mode shapes in all three planes. The resulting identifiable mode shapes are described. The most affected mode is Coordinated Mode 2 (Baseline Peak 14 and Damaged Peak 11): this heavily coupled mode is softened by 19.42%. However, not all peaks shift downwards, but the differences are within a fairly reasonable 5%.

Table 1. Coordinated modes for tri-axial accelerometer data.

Baseline		Damaged Case		% Diff.	Mode Shape Description		
Peak #	Freq. (Hz)	Peak #	Freq. (Hz)		XY	YZ	XZ
4	9.336	4	9.688	3.77	Y translation	-	-
14	60.938	11	49.102	-19.42	Torsion about Z, Y Translation	Torsion about X	-
16	80.586	13	76.641	-4.90	Torsion about Z	Torsion about X	-
18	108.086	15	100.000	-7.48	-	Torsion about X	Bending about Y
19	120.586	16	121.055	0.39	Torsion about Z, Y Translation	-	Bending about Y
22	145.664	17	138.164	-5.15	Torsion about Z	Translation in Z	Bending about Y
23	173.477	18	180.898	4.28	-	Torsion about X	Vague bending about Y
26	201.016	19	201.367	0.17	Torsion about Z	Torsion about X	Bending about Y
28	215.938	20	209.258	-3.09	-	Torsion about X	Bending about Y

These nine coordinated modes were then fed into the next SHM[TM] step of calculating damage indices. Four damage indication algorithms were employed to locate damage, and visual interpretations were generated for each. Recall that the rubber bearing was inserted at the top of the right-hand pier, so successful identification would show some pattern of damage with a maximum along the right boundary line.

Coordinated Modal Assurance Criterion (COMAC) is a fairly common means of comparing two mode shapes. The tri-axial accelerometer data is mined to produce damage detection plots for each direction independently. The y-direction result often indicates the most damage as sidesway is the fundamental mode. Yet, in order to compare with the LDV results, the z-direction results must be utilized as represented in Figure 19.
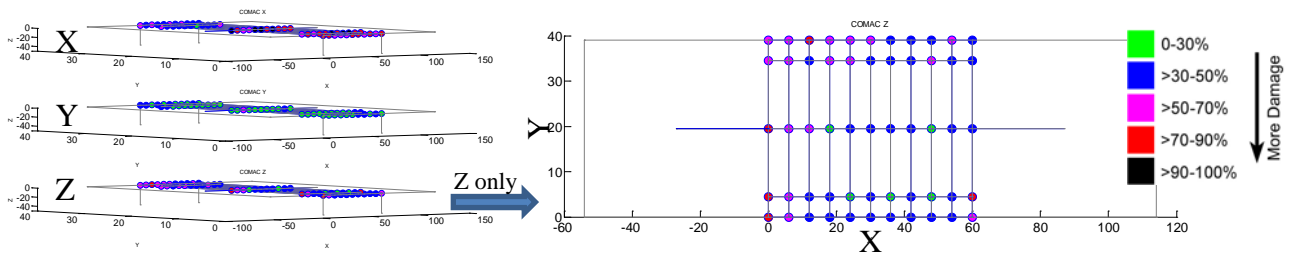
Figure 19. Damage detection using COMAC on tri-axial (left) and z-direction (right) accelerometer data.

The color scheme is normalized with respect to the maximum damage value in any direction and thus shows the percent of overall induced relative damage – not absolute damage as in a "safe" threshold. Even so, the damage is shown is a relatively diagonal pattern, indicating that torsion is quite dominant. Both boundaries indicate damage, but the greater effect exists at the left edge rather than the right pier. Five points of 70-90% damage are identified (with four of them along the left edge), so an inspector may be able to know something has changed in a boundary. False positives are at a minimum in this metric.

COMAC was also applied to mode shape curvature, or point-by-point numerical second derivative. The tri-axial accelerometer data is again mined to produce damage detection plots for each direction independently, and the z-direction results are shown in Figure 20. All points show at least 50% damage, but this is with respect to values in all three directions. Although there are no blue or green nodes, the black nodes are still at least 20% more damaged than the magenta nodes. No trend behavior is evident, except perhaps the slab's center in spared some damage. An inspector would have no idea where to investigate and might even panic seeing so many false positives. This indicator appears too sensitive in this case.
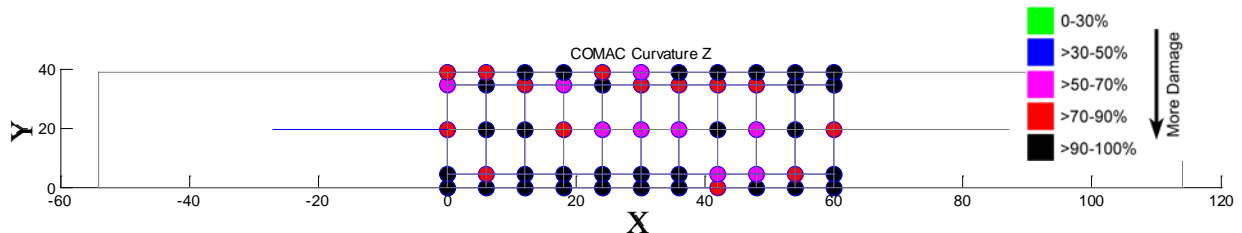
Figure 20. Damage detection using COMAC of mode shape curvature on z-direction accelerometer data.

Mode shape curvature is also used as an indicator through proportional analysis, here direct division. A damaged mode shape's curvature is point-by-point divided by the associated baseline mode shape's curvature. Using this scheme, the tri-axial accelerometer data is mined to produce damage detection plots for each direction independently, and the z-direction results are shown in Figure 21. The variation in this indicator's magnitude is extreme, generating in a large disparity between maxima and minima. This results in a plot that shows little or no damage pattern, only singularities that could be false readings rather than trend behavior. An inspector might have false confidence, believing so many potentially false negatives.
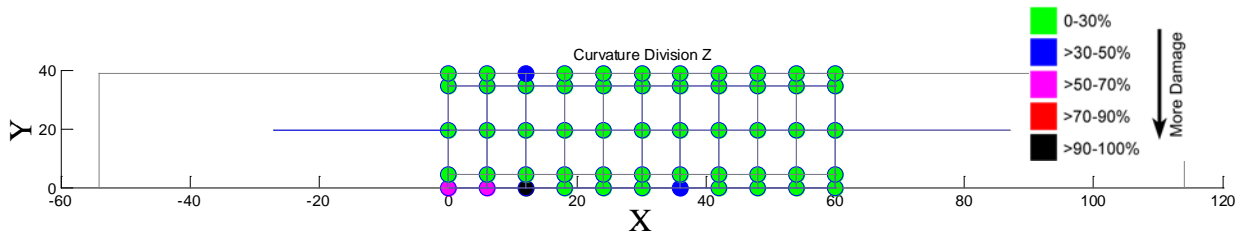
Figure 21. Damage detection using mode shape curvature division on z-direction accelerometer data.

The flexibility of a structure can be proportionally estimated from two cross-correlated output signals. This is another means of comparing baseline to damaged mode shapes via standard deviation, creating the Normalized Flexibility Index. The tri-axial accelerometer data is mined to produce damage detection plots for each direction independently. To directly compare with the LDV data's plots, z-direction results are provided in Figure 22. The three-step color scheme is based upon the number of standard deviations away from the center of the bell curve. This plot shows no discernible damage pattern, and the least softened right edge is where the artificial damage was inflicted. An inspector would certainly not know where to investigate further.
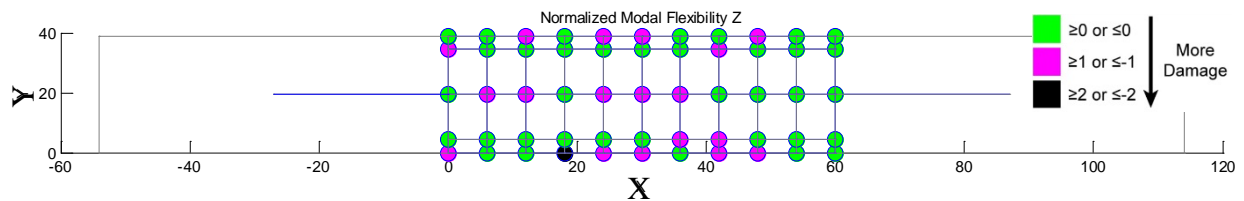
Figure 22. Damage detection using Normalized Modal Flexibility on z-direction accelerometer data.

Previous studies on the same concrete bridge showed this flexibility metric to be a reasonable indicator in the lateral y-direction: here, the sway direction has a slightly better but still appears poor. This led to re-investigation of the coordinated modes. The mean strain energy variation when all nine modes were included was 17.72; including only the three best matching modes, the value was 0.55, showing less skew. This desirable result led to repeating the four damage detection plots with just the three main coordinated modes in Table 2.

Table 2. Reduced coordinated modes for tri-axial accelerometer data.

Baseline		Damaged Case		%	Mode Shape Description		
Peak #	Freq. (Hz)	Peak #	Freq. (Hz)	Diff.	XY	YZ	XZ
4	9.336	4	9.688	3.77	Y translation	-	-
18	108.086	15	100.000	-7.48	-	Torsion about X	Bending about Y
26	201.016	19	201.367	0.17	Torsion about Z	Torsion about X	Bending about Y

The result for the COMAC on the reduced modes (Figure 23) provides less range and less trend behavior. False positives are still minimal, but no clear severe damage is shown. Thus, using the reduced mode degrades the COMAC metric's accuracy. COMAC on mode shape curvature provides much improved range and less false positives. Still, no trend behavior is evident in Figure 24. The reduction in coordinating modes further demonstrates that curvature division is a weak indicator: in Figure 25, the false negatives still exist and the positive singularities moved. Lastly, the Normalized Modal Flexibility plot of Figure 26 shows little difference with the reduced modes.

In short, the reduced number of coordinate modes provided no major improvement of these results. It is more likely that the dominance of the y-direction sidesway has more effect.
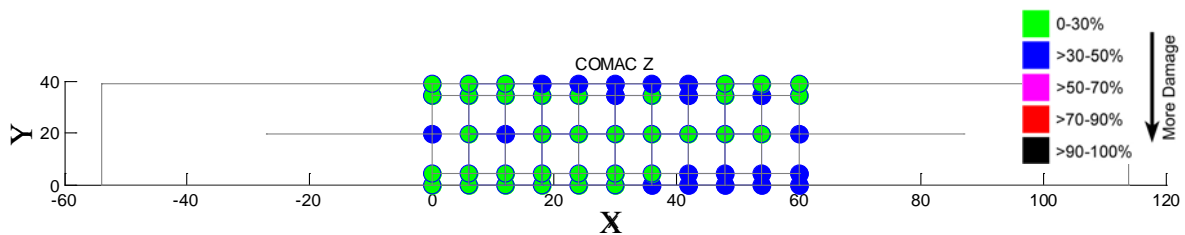
Figure 23. Damage detection using COMAC on reduced z-direction accelerometer data.

Figure 24. Damage detection using COMAC of mode shape curvature on reduced z-direction accelerometer data.

34

Figure 25. Damage detection using mode shape curvature division on reduced z-direction accelerometer data.

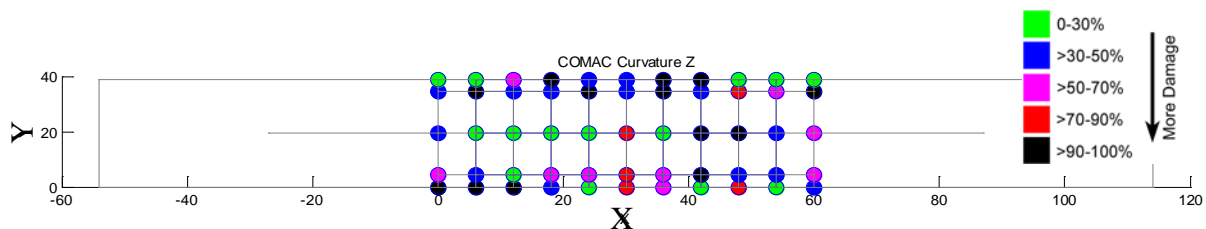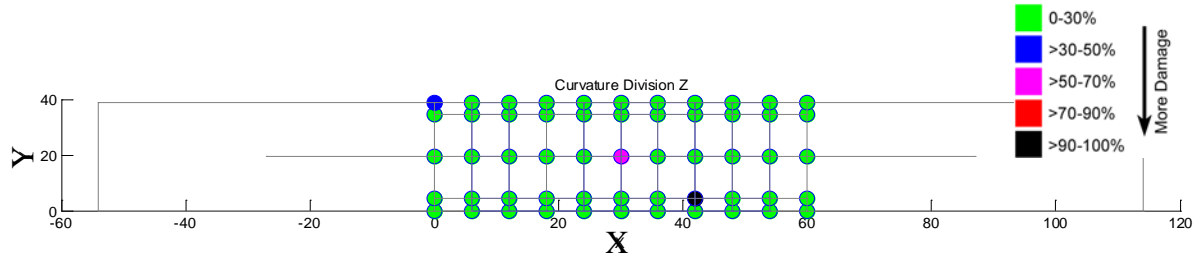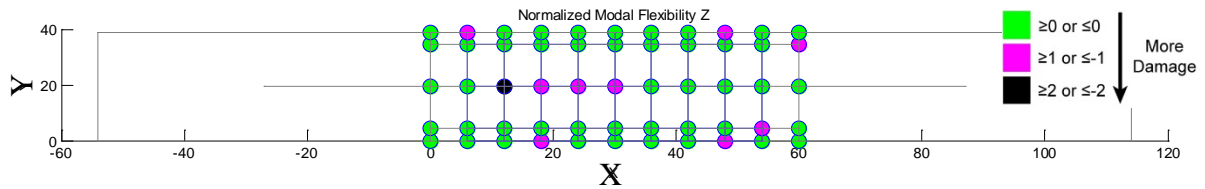**Figure 26. Damage detection using Normalized Modal Flexibility on reduced z-direction accelerometer data.**

<u>Damage Detection Results</u>: LDV Data

The cumulative frequency response functions (FRFs) are provided in Figure 27. These traces are the summation of all 45 data points in one vertical channel for a total of 45 time histories. The damaged trace's peaks show shifting and softening over 100 Hz, but the comparison less than 85 Hz is more difficult as illustrated in the zoomed view in Figure 28.

Comparison of the mode shapes reveals the coordinated modes of Table 3. Using the YZ and XZ views, the baseline mode shapes have been compared to those of the damaged case. The resulting nineteen mode shapes are not physically describable as the true coupling nature is not captured with a single axis.

The average difference is -4.32% with a standard deviation of 0.045, and all but three natural frequencies decreased, demonstrating softening. Baseline Peaks 44 and 50 are outliers showing the most damage at -12.57% and -17.87%, respectively. Thus, large frequency shifts are shown in the mid-range 110 Hz to 190 Hz. Examination of the FRFs also reveals those peaks dropped markedly in amplitude and increased in breadth. Baseline Peak 7 increased by 3.08%, which is within a reasonable range for variable contact behavior.

Table 3. Coordinated modes for LDV data.

Baseline		Damaged Case		% Diff.
Peak #	Freq. (Hz)	Peak #	Freq. (Hz)	
3	10.464	7	9.839	-5.97
4	11.870	8	11.089	-6.58
7	16.477	11	16.985	3.08
8	20.577	13	20.460	-0.57
10	22.880	14	22.451	-1.88
14	28.620	17	26.160	-8.59
15	30.611	19	30.104	-1.66
16	32.798	20	31.587	-3.69
17	34.867	21	33.657	-3.47
26	53.765	29	48.650	-9.51
27	58.841	31	57.279	-2.65
28	61.496	32	58.802	-4.38
30	67.157	34	66.806	-0.52
32	71.023	35	73.092	2.91
35	80.589	37	81.955	1.70
40	120.415	45	110.068	-8.59
44	141.929	46	124.085	-12.57
50	185.034	47	151.963	-17.87
59	252.777	54	249.654	-1.24

Of the total 119 peaks, the nineteen coordinated mode sets were then fed into the next SHM^{TM} step of calculating damage indices. Four damage indication algorithms were employed to locate damage, and visual interpretations were generated for each. Again, the rubber bearing was inserted at the top of the right-hand pier, so successful identification would show some pattern of damage with a maximum along the right boundary line.

Note that the mean strain energy variation when all nineteen modes were included was 8.680, which shows less skew than the nine mode acceleration data set. The carefully coordinated modes from the LDV show better grouping and increased numbers, but the true test is whether damage is better located.
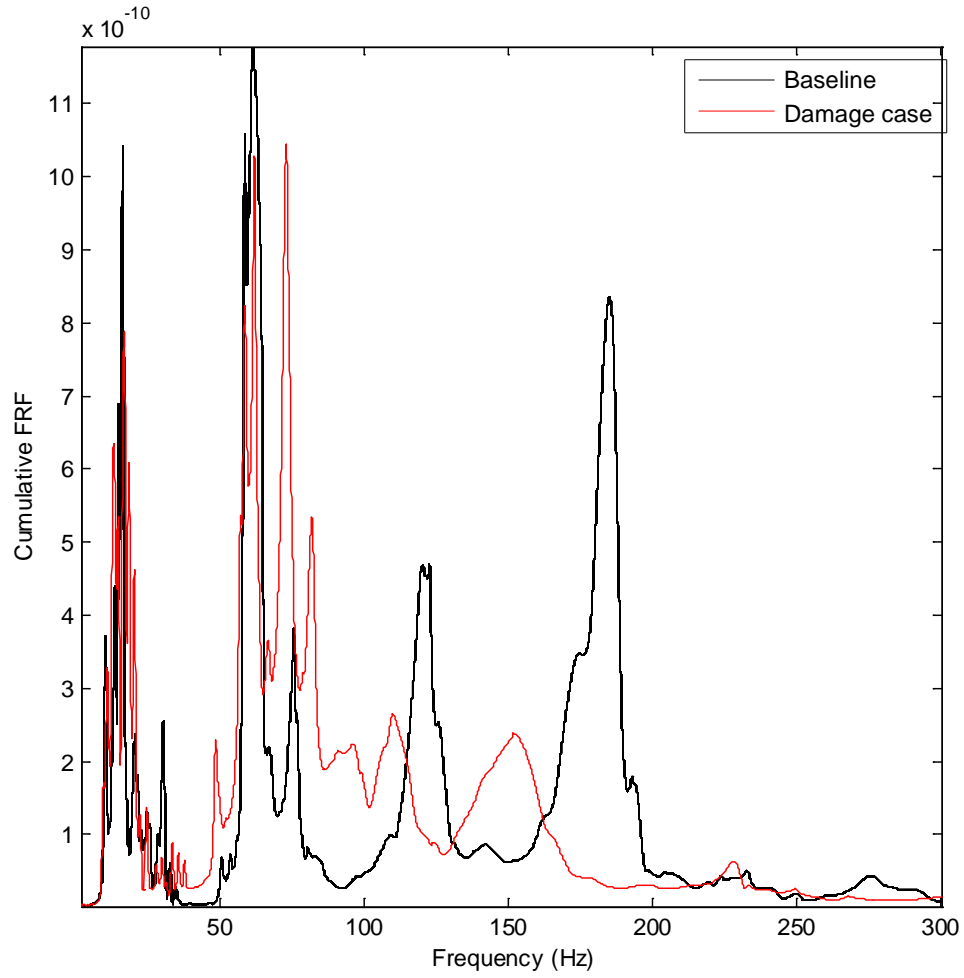
**Figure 27. Non-normalized cumulative FRFs using LDV data.**
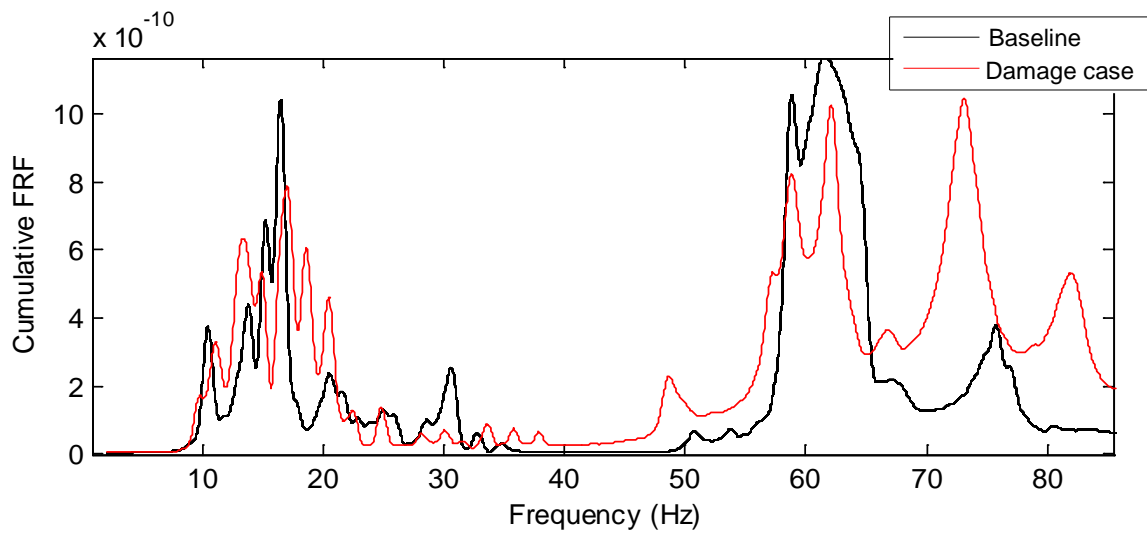
Figure 28. Zoom of Figure 27: non-normalized cumulative FRFs using LDV data.

The vertical LDV data was mined to produce a damage detection plot using COMAC. Figure 29 illustrates a damage pattern that is more erratic than that obtained with the accelerometer data. The indication of most damaged three-node line at the slab's center is not possible. The left edge does show more damage than the right as prior studies, but not as induced.
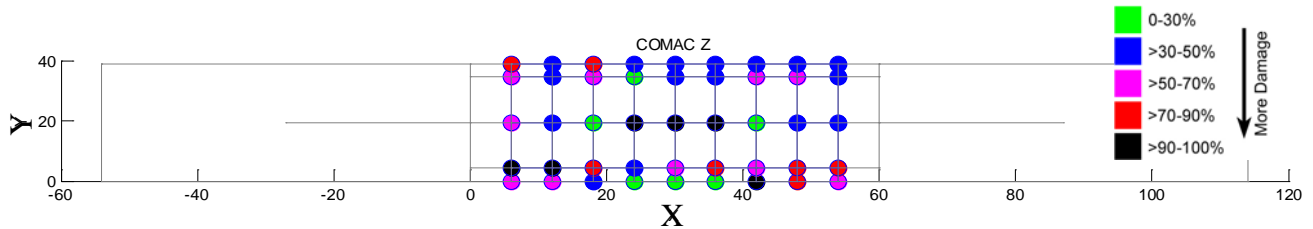
Figure 29. Damage detection using COMAC on LDV data.

As plotted in Figure 30, COMAC on mode shape curvature employing the LDV data provides better range of damage index values. No trend behavior is evident, but the pattern is somewhat similar to that with the accelerometer data. This metric again shows too much damage, and an inspector would have no idea where to investigate due to such high sensitivity.
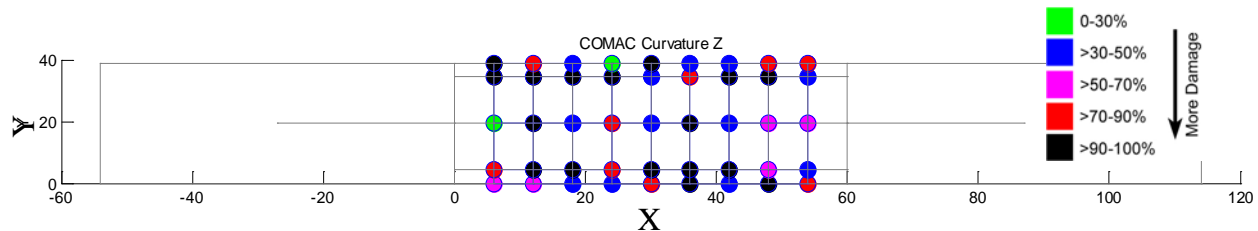
Figure 30. Damage detection using COMAC of mode shape curvature on LDV data.

Direct division on mode shape curvature for the LDV data again provided extreme variations in magnitude. Figure 31 depicts a plot that shows no damage pattern, only singularities that could be false readings rather than trend behavior. These singularities are not the same nodes as those using the accelerometer data. An inspector might have false confidence or panicked inspection at an incorrect location.
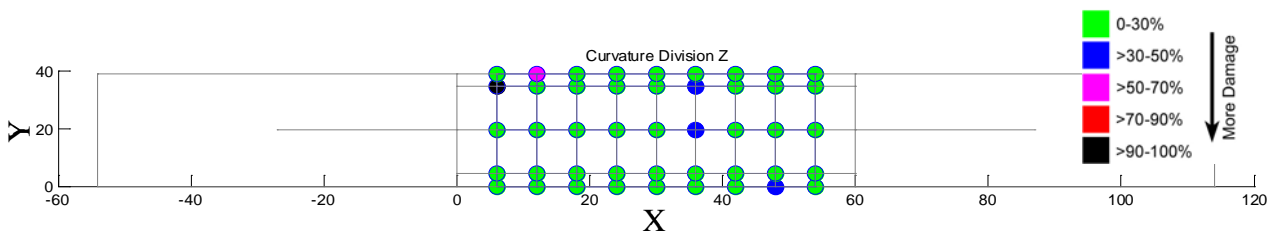
Figure 31. Damage detection using mode shape curvature division on LDV data.

The Normalized Flexibility Index algorithm applied to the LDV data results in Figure 32. As that with the accelerometer data, this plot shows no discernible damage pattern. Perhaps an inspector's imagination would lead him to investigate the *y=0* line, but the result is certainly no better than that with contact sensor measurements.
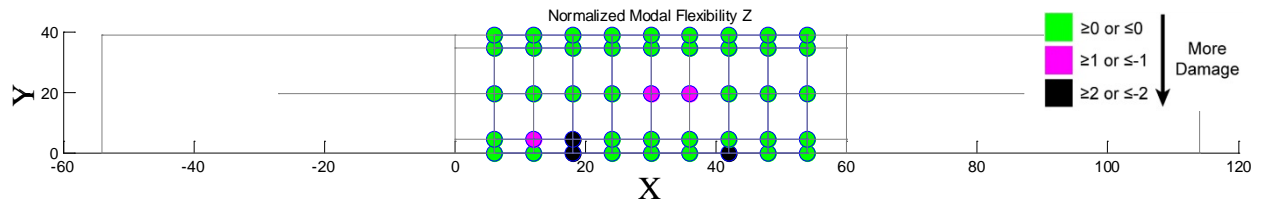
Figure 32. Damage detection using Normalized Modal Flexibility on LDV data.

In summary, these plots appear qualitatively similar to those from the accelerometer data despite the significant differences in the frequency content (both numbers and locations of peaks). The coordinated modes are more numerous for the LDV data due to the increased sensitivity; however, the effect on damage detection plotting is insignificant. Reducing the number of considered modes is also unlikely improve these plots since it did not for the accelerometer data. Furthermore, it is difficult to determine which matched modes should be included. With no physical sense due to the single-dimensional analysis, the choice appears arbitrary. One hypothesis would be to separately consider each rather subjective frequency range.

CONCLUSIONS

Regarding accelerometer data, current results can be compared to the previous NCITEC 2012 study. The previous Baseline and Asymmetrical Damage Case 3 represent equivalent induced damage as the current study's two cases. Results are published in Appendix D of Steven Worley's M.S. thesis, and an article has been submitted to the Journal of Bridge Engineering.

Modal coordination has improved. In the previous study, five coordinating modes were identified, but nine were found herein. Literature reviews reveal the greatest number of coordinated modes from experimentally captured data to be three, so both NCITEC studies are significant. As presented in Table 4, the previous baseline frequencies are slightly lower than those comparable for the current baseline: the concrete connections have softened by several slab removal and replacements during test series.

Table 4. NCITEC 2012 baseline versus NCITEC 2014 baseline.

Prior Baseline Frequency (Hz)	Current Baseline Frequency (Hz)	% Difference	Modal Description
12.23	9.34	-30.94	Translation
64.17	60.94	-5.30	Rotation & Translation
114.63	108.09	-6.05	Rotation & Bending
153.83	145.66	-5.61	Bending & Translation
224.41	215.94	-3.92	Rotation & Bending

Considering damage location plotting, a reduced number of coordinated modes did not appear to affect damage detection. If inaccurate mode coordination were a problem, this exercise would have generated clearer detection plots; however, no improvement resulted. Thus, the damage index algorithms appear to be the best concentration of future research.

As further evidence, the damage detection conclusions of the NCITEC 2012 project varied from those in this work despite testing on the same reinforced concrete bridge. The best detection index herein is COMAC using all nine coordinated modes using tri-axial accelerometer data. Figure 33 shows the prior result (33a) and the vast improvement in the current work (33b). The damage pattern in the z-direction is far improved by illustrating boundary condition changes; torsion and asymmetry remain evident. The 2012 study showed similar results for the y-direction using the Damage Location Vector algorithm, which was not employed herein.   Very similar and quite inaccurate results were obtained in NCITEC 2012 and 2014 for COMAC on curvature and curvature division. The Normalized Modal Flexibility Index worked well for some directions of asymmetrical damage cases in the 2012 study, so this metric cannot be excluded although inaccurate herein. Lastly, the strain energy content was very different, so further study is required.
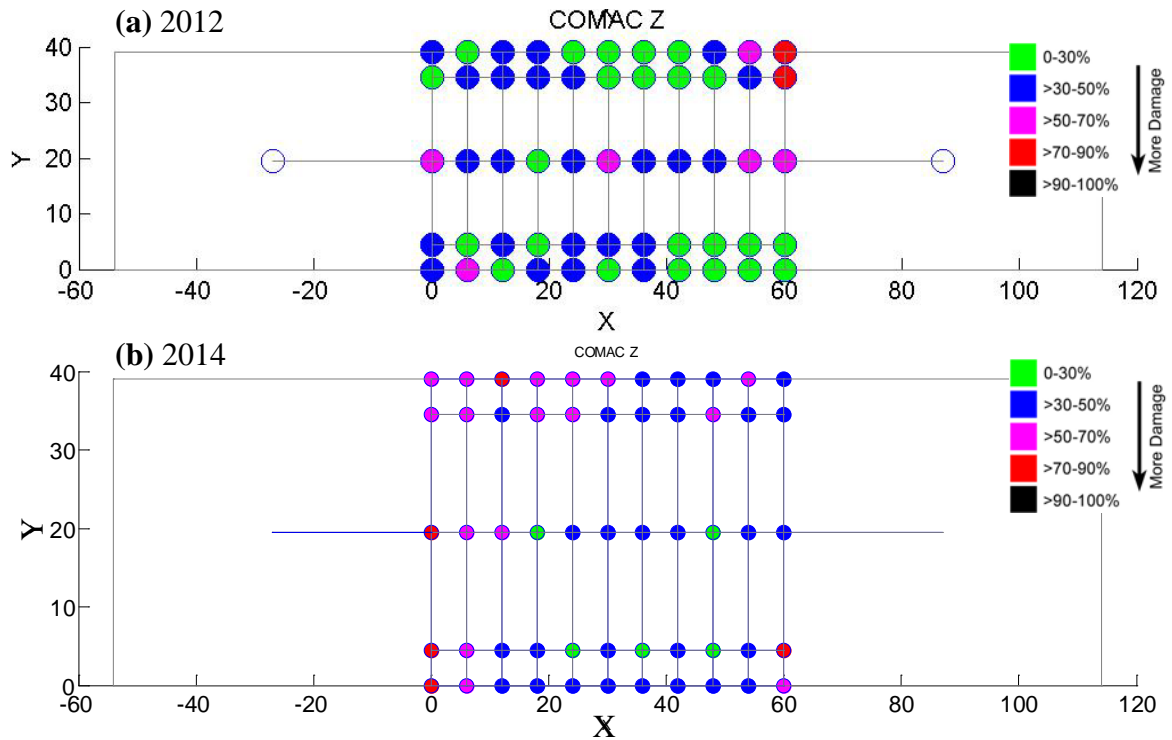
Figure 33. Damage detection using COMAC on z-direction accelerometer data from (a) 2012 and (b) 2014.

Regarding LDV data, damage detection results were qualitatively similar to those with only vertical accelerometer data. The positive aspect is that similar performance implies that either sensing means will work. However, the LDV results are more difficult to interpret, especially below 100 Hz. The increased sensitivity results in more peaks, which requires more human judgment – a potential weakness for rail and road bridges, which have natural frequencies in the most turbulent LDV frequency range. Most literature studies cannot find enough modes to coordinate, but it seems the LDV setup provides too many similar modes. The LDV data did provide more coordinated modes and similar detection plots, but not necessarily successful damage location. Another indicator successful in NCITEC 2012, the Damage Location Vector algorithm may be useful but was not applicable herein due to so much variation in frequency content.

The major strength of non-contact laser measurement is conversely balanced by the main weakness of single axis data capture. True structures are heavily coupled, requiring a three-dimensional understanding. In this work, direct mode shape comparisons to those from accelerometer measurements were consequently not possible. Horizontal measurements were also captured, but these are global rather than point-by-point, as needed for damage location plots. Even if a flange were glued to the bridge for capture, its response would cause interference. A far more expensive setup of multiple scanning LDV would still miss some direction for an interior point. In short, optical methods have their spatial limitations.

Regarding LDV data, damage detection results were qualitatively similar to those with only vertical accelerometer data. The positive aspect is that similar performance implies that either sensing means will work. However, the LDV results are more difficult to interpret, especially below 100 Hz. The increased sensitivity results in more peaks, which requires more human judgment – a potential weakness for rail and road bridges, which have natural frequencies in the most turbulent LDV frequency range. Most literature studies cannot find enough modes to coordinate, but it seems the LDV setup provides too many similar modes. The LDV data did provide more coordinated modes and similar detection plots, but not necessarily successful damage location. Another indicator successful in NCITEC 2012, the Damage Location Vector algorithm may be useful but was not applicable herein due to so much variation in frequency content.

The major strength of non-contact laser measurement is conversely balanced by the main weakness of single axis data capture. True structures are heavily coupled, requiring a three-dimensional understanding. In this work, direct mode shape comparisons to those from accelerometer measurements were consequently not possible. Horizontal measurements were also captured, but these are global rather than point-by-point, as needed for damage location plots. Even if a flange were glued to the bridge for capture, its response would cause interference. A far more expensive setup of multiple scanning LDV would still miss some direction for an interior point. In short, optical methods have their spatial limitations.

RECOMMENDATIONS

The determination of any damage threshold is an actively pursued research topic and is extremely complex for civil infrastructure. Thus, this project has increased the base of knowledge for low frequency structures. However, much more work is needed before an inspection tool is developed. The developed method will apply to broad classifications of structures and will significantly improve current infrastructure management. This methodology will apply to both railroad and highway bridges (both passenger and freight) as well as potentially extending to dams, levees, buildings, etc. The eventual goal is to provide condition-based maintenance via a cost-effective product that will transverse any structure and identify an overall change in its stiffness, indicating that localized inspection is required before a bridge collapse, for instance.

The potential outcomes are more pointed inspections and condition-based maintenance rather than time-based maintenance. The ideal results would be a method of speedy non-contact inspections that can evaluate internal structural damage. Once the new technique is finalized, D.O.T. inspectors will need training in quantitative structural deterioration measurements.

State D.O.T.s and regional construction firms have been contacted by the PI for input, including both technical as well as advice on to how best to transfer any new technique to field inspectors. The only obtained feedback thus far has been through the Ole Miss Alumni Association. Also note that user friendly software is in development, and a proposal has been submitted to and rejected by the FHWA.

From the results of this and the prior project, several recommendations can be made regarding LDV use for infrastructure inspection. Low grazing angles and filtering cannot be used. It is also best for the LDV beam to coincide with vibration component of interest. The LDV must be mounted on a mechanically stable platform, and any natural frequencies of the platform must be isolated before signal post-processing. Corroded or dirty members may require surface conditioning or a more powerful LDV.

Research is proceeding towards finding the damage indicators that work best for different classes of structures. The health program outputs several different metrics, but which (or which combination) is preeminent for any bridge or even any structure. Various materials and geometries are also expected to affect damage detection. Once the most effective indication method is selected, the damage thresholds need identification for decision-making. Safety thresholds can then be used for maintenance decision-making.

ACRONYMS, ABBREVIATIONS, AND SYMBOLS

COMAC	Coordinate Modal Assurance Criteria
DAQ	Data acquisition system
DOT	Department of Transportation
FFT	Fast Fourier transform
FHWA	Federal Highway Administration
FRF	Frequency response function
LDV	Laser Doppler Vibrometer
MAC	Modal Assurance Criteria
NCPA	National Center for Physical Acoustics
NI	National Instruments
PC	Personal computer
RC	Reinforced concrete
SHE^{TM}	Structural Health Evaluation (trademarked)
SHM	Structural Health Monitoring
UM	The University of Mississippi
3D	Three-dimensional

REFERENCES

1. T. Miyashita, H. Ishii, Y. Fujino, A. Shoji, M. Seki, "Clarification of the Effect of High-Speed Train Induced Vibrations on a Railway Steel Box Girder Bridge Using Laser Doppler Vibrometer," *Experimental Vibration Analysis for Civil Engineering Structures* (2005), 349-357.
2. Przemysław Kołakowski, Jacek Szelążek, Krzysztof Sekuła, Andrzej Świercz, Krzysztof Mizerski and Piotr Gutkiewicz, "Structural health monitoring of a railway truss bridge using vibration-based and ultrasonic methods," *Smart Materials and Structures*, 20 No. 3 (2011).
3. Davood Rezaei and Farid Taheri, "A novel application of a laser Doppler vibrometer in a health monitoring system," *Journal of Mechanics of Materials and Structures*, Vol. 5 (2010), No. 2, 289–304.
4. Hani H. Nassifa, Mayrai Gindyb, Joe Davis, "Comparison of laser Doppler vibrometer with contact sensors for monitoring bridge deflection and vibration," *NDT&E International* 38 (2005) 213–218.
5. Y. Fujino, D.M. Siringoringo, T. Nagayama & D. Su, "Control, simulation and monitoring of bridge vibration – Japan's recent development and practice for monitoring bridge deflection and vibration," IABSE-JSCE Joint Conference on Advances in Bridge Engineering-II, August 8-10, 2010, Dhaka, Bangladesh. ISBN: 978-984-33-1893-0, Amin, Okui, Bhuiyan (eds).
6. Takeshi Miyashita, and Masatsugu Nagai, "Vibration-based Structural Health Monitoring for Bridges using Laser Doppler vibrometers and MEMS-based Technologies," *Steel Structures* 8 (2008) 325-331.
7. V. Aranchuk, A.Lal, C. Hess, and J.M. Sabatier, "Multi-beam laser Doppler vibrometer for landmine detection," *Optical Engineering*, 45 (10), October 2006.
8. Amit Lal, Slava Aranchuk, Valentina Doushkina, Ernesto Hurtado, Cecil Hess, Jim Kilpatrick, Drew L'Esperance, Nan Luo, Vladimir Markov, Jim Sabatier, Eddie Scott, "Advanced LDV instruments for buried landmine detection," *Proceedings of the SPIE*, Vol. 6217, 621715 (2006).
9. Vyacheslav Aranchuk, Amit K. Lal, Hansheng Zhang, Cecil F. Hess, and James M. Sabatier, "Acoustic Sensor for Landmine Detection using a Continuously Scanning Multi-Beam LDV," *Proceedings of the SPIE*, Vol. 5415, 61-69 (2004).
10. Vyacheslav Aranchuk, James M. Sabatier, Amit K. Lal, Cecil F. Hess, Richard. D. Burgett , and Michael O'Neill, "Multi-beam laser Doppler vibrometry for acoustic landmine detection using airborne and mechanically-coupled vibration," *Proc. SPIE*, Vol. 5794, 624-631 (2005).
11. V. Aranchuk; A. K. Lal; C. F. Hess; J. M. Sabatier; R. D. Burgett; I. Aranchuk; W. T. Mayo, "Speckle noise in a continuously scanning multibeam laser Doppler vibrometer for acoustic landmine detection", *Proceedings of the SPIE*, Vol. 6217, p.621716-1 - 621716-1, 2006.
12. Richard Burgett, Vyacheslav Aranchuk, and Ina Aranchuk, "Experimental investigation of buried landmine detection using time division multiplexing of multibeam laser Doppler vibrometer channels", *Proceedings of the SPIE*, Vol. 8357, 83570H-1, Orlando, April 2012.

13. James Sabatier, Vyacheslav Aranchuk, Alexander Ekimov, and Ina Aranchuk "Application of multiple beam laser Doppler vibrometry for passive tunnel detection," *Proc. of the Military Sensing Symposium on Battlespace Acoustic and Seismic Sensing, Magnetic and Electric Field Sensors* (2009).

14. Vyacheslav Aranchuk and James Sabatier, " Sensing foliage vibration caused by sound from a obscured vehicle using a laser Doppler vibrometer: effect of multiple objects." *Proc. of the Military Sensing Symposium on Battlespace Acoustic and Seismic Sensing, Magnetic and Electric Field Sensors* (2010).

15. Vyacheslav Aranchuk, James Sabatier, Alexander E. Ekimov, and Richard Mack , "Standoff detection of obscured vehicle with laser Doppler vibrometer," *Proceedings of the SPIE* 73030H-1 (2009).

16. http://www.cinewsnow.com/news/road-construction/I-55-Bridge-Work-Will-Slow-Traffic-South-117115878.html (accessed 3/9/13).

APPENDIX

Text data was logged during this report. Data is stored for each experimental efforts, and the PI is maintaining copies for a minimum of five years. Any requests for the data should be directed to Dr. Ervin at eke@olemiss.edu.

Additional information can be obtained from the publications resulting from this grant. Cumulative external citations are as follows:

Steven B. Worley, "Development and Validation of the Structural Health Evaluation (SHE^{TM}) Program," Master's Thesis, August 2014. Successfully defended May 2014.

Elizabeth K. Ervin, "Three Experimental Applications of Health Algorithms to Improve Infrastructure Inspection," European Workshop on Structural Health Monitoring, July 2014. Abstract accepted. Presentation in July 2014.

Steven B. Worley and Elizabeth K. Ervin, "Structural Health Indication on a Reinforced Concrete Test Bridge with Pier Damage," ASCE Journal of Bridge Engineering (submitted December 8, 2014).

Steven B. Worley and Elizabeth K. Ervin, "Considerations on Vibration Testing Techniques of an In-service Highway Bridge," ASCE Journal of Highway and Transportation Research and Development (in final preparation).

Vyacheslav Aranchuk and Elizabeth K. Ervin, "Dynamic Evaluation of Structural Integrity of Railway Tracks using Laser Doppler Vibrometry," NDT & E International (in preparation).